Thermoelectric power of the YbT_2Zn$_{20}$ (T = Fe, Ru, Os, Ir, Rh, and Co) heavy fermions

E. D. Mun,* S. Jia,† S. L. Bud'ko, and P. C. Canfield

Ames Laboratory, U.S. Department of Energy and Department of Physics and Astronomy, Iowa State University, Ames, Iowa 50011, USA

(Received 22 July 2010; published 10 September 2012)

The thermoelectric power, $S(T)$, of the heavy fermions YbT_2Zn$_{20}$ (T = Fe, Ru, Os, Ir, Rh, and Co) has been measured to shed further light on their strong electronic correlations. A large, negative, local minimum in $S(T)$ with approximately $-70\ \mu$V/K is found for all compounds. From the observed local minimum, the energy scales associated with both the Kondo temperature and the crystalline electric field splitting are deduced and compared to previous specific heat measurements. At low temperatures, a highly enhanced $S(T)/T$ value is observed for all members, although $S(T)$ does show a deviation from a purely linear temperature dependence, $S(T) = \alpha T$, for $T \neq$ Fe members. In the zero-temperature limit, estimated by a simple linear extrapolation, the enhanced $S(T)/T$ value strongly correlates with the electronic specific heat coefficient, $C(T)/T$.

DOI: 10.1103/PhysRevB.86.115110 PACS number(s): 72.15.Jf, 72.15.Qm, 75.20.Hr, 75.30.Mb

I. INTRODUCTION

In a heavy fermion (HF) Kondo lattice system, the ground state is a Fermi-liquid (FL) state formed out of Landau quasiparticles. In Ce-, Yb-, and U-based intermetallic systems the conduction electrons compensate, or screen, the localized moments of the f electrons where localized electrons together with their screening cloud form quasiparticles. These quasiparticles have heavy masses, reflected in an enhanced value of the Sommerfeld coefficient, $\gamma = C(T)/T|_{T\to 0}$, at low temperatures.[1]

For Yb-based HF systems, the electrical resistivity and thermoelectric power (TEP) reveal complex temperature dependencies with local extrema. In general, these extrema are related to Kondo scattering associated with the ground state and excited states of the crystalline electric field (CEF) energy levels.[2–4] The characteristic temperatures of the local maximum shown in $\rho(T)$ and the local minimum developed in $S(T)$ allow for an estimate of the Kondo temperature, T_K, and the CEF splitting, Δ/k_B, as relevant energy scales in Yb-based HF systems.

The FL state in HF Kondo lattice systems shows strong correlations among physical quantities. One such correlation is the Kadowaki-Woods (K-W) ratio, a relation between the electrical resistivity [$\rho(T) - \rho_0 = AT^2$] and specific heat [$C(T) = \gamma T$], given by what was originally thought to be a universal ratio $A/\gamma^2 = 1.0 \times 10^{-5}\ \mu\Omega\ \text{cm/(mJ/mol K)}^2$.[5,6] Recently, systematic deviations of the K-W ratio in many HF systems (especially for Yb-based compounds) have been explained by taking into account the ground-state degeneracy ($N = 2j + 1$).[7–9] A FL state is also characterized by the Wilson ratio (R_W) which links γ to the Pauli susceptibility $\chi(0)$,[10–12] which is given by $R_W = \pi^2 k_B^2 \chi(0)/[j(j+1)g^2\mu_B^2\gamma^2]$, where k_B, g, and μ_B are the Boltzman constant, Lande's factor, and Bohr magneton, respectively.[1] In addition to the R_W and the K-W ratio, the zero-temperature limit of the TEP divided by temperature, $S(T)/T = \alpha$, for several correlated materials has shown a strong correlation with γ via the dimensionless ratio $q = N_A e S/\gamma T = N_A e\alpha/\gamma$,[13] where N_A is the Avogadro number and e is the carrier charge. It is very important to test the universality of the K-W ratio, Wilson's number, and the q ratio for a number of isostructural materials; the YbT_2Zn$_{20}$ compounds offer six isostructural materials where the local environment of the hybridizing Yb ion is identical (nearest and next-nearest neighbors are all Zn).

In this paper, TEP measurements on YbT_2Zn$_{20}$ (T = Fe, Ru, Os, Ir, Rh, and Co) are presented as functions of temperature and magnetic field to study their temperature and magnetic field dependence and to evaluate the correlation between specific heat and TEP in the zero-temperature limit. These compounds crystallize in the cubic $CeCr_2Al_{20}$-type structure ($Fd\bar{3}m$, No. 227)[14] and have been reported to be HF metals with no long-range order down to 20 mK.[15] In the FL regime it has been shown that the R_W and K-W ratios in this family follow the theoretical predictions with different ground-state degeneracies. The TEP data of YT_2Zn$_{20}$ (T = Fe, Co) are also presented for comparison. YFe_2Zn_{20} is an example of a nearly ferromagnetic Fermi liquid (NFFL) with a highly enhanced magnetic susceptibility value at low temperatures,[16] whereas YCo_2Zn_{20} shows unenhanced Pauli paramagnetic, metallic behavior.

II. EXPERIMENTAL

Single crystals of YbT_2Zn$_{20}$ (T = Fe, Ru, Os, Ir, Rh, and Co) and isostructural YT_2Zn$_{20}$ (T = Fe and Co) were grown out of excess Zn[15,16] using standard solution growth techniques.[17,18] The TEP was measured using a dc, alternating heating technique that utilizes two heaters and two thermometers.[19] A Quantum Design Physical Property Measurement System provided the temperature (from 2 to 300 K) and magnetic-field (up to 140 kOe) environment. For T = Fe, Rh, and Co, zero field TEP measurements were extended down to 0.4 K, measured using the same technique,[19] in a CRYO Industries of America ^{3}He system. The heat current was generated in the (111) plane of the samples [$\Delta T \parallel (111)$] and the magnetic field was applied along the [111] direction maintaining a transverse configuration, $\Delta T \perp \mathbf{H}$.

III. RESULTS

Figure 1 shows the TEP data for YFe_2Zn_{20} and YCo_2Zn_{20}. The temperature-dependent TEP, $S(T)$, of these compounds is similar to normal metallic systems. At 300 K, $S(T)$ of both compounds is positive and has an absolute value of $\simeq 9\ \mu$V/K for YFe_2Zn_{20} and $\simeq 5\ \mu$V/K for YCo_2Zn_{20}, and then decreases

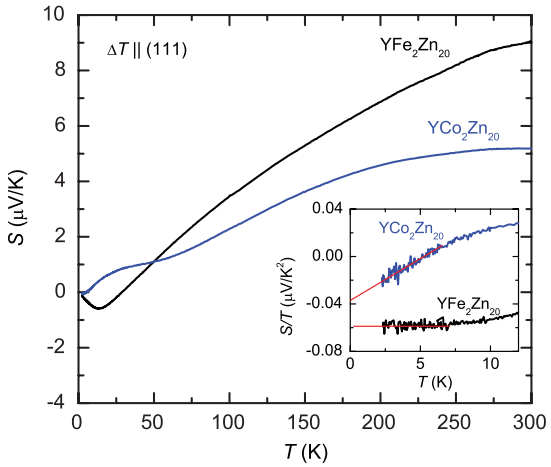

FIG. 1. (Color online) Temperature-dependent thermoelectric power, $S(T)$, of YFe_2Zn_{20} and YCo_2Zn_{20} for $\Delta T \parallel (111)$. Inset: $S(T)/T$ vs T below 12 K. Solid lines are a guide to eye.

monotonically to below 50 K with decreasing temperature. With further cooling, $S(T)$ of YCo_2Zn_{20} passes through a broad peak ($\sim\Theta_D/12$,[20] where Θ_D is the Debye temperature) expected to be due to phonon drag.[21] On the other hand, $S(T)$ of YFe_2Zn_{20} shows a local minimum around 14 K ($\sim\Theta_D/23$[20]) that is not currently understood. The absolute value of the TEP for YFe_2Zn_{20} is much smaller than other NFFL systems. A signature of the spin fluctuation temperature, T_{sf}, has been inferred from a shoulder in AFe_4Sb_{12} (A = Ca, Sr, and Ba) data[22] and as a minimum developed in RCo_2 (R = Y, Sc, and Lu) data.[23] The minimum developed near 14 K may be related to the signature of spin fluctuation, combined with phonon drag in the YFe_2Zn_{20} system. In the $T \rightarrow 0$ K limit, the magnitude of $S(T)/T$ of YFe_2Zn_{20} is larger than that of YCo_2Zn_{20} as shown in the inset of Fig. 1.

The zero field $S(T)$ data of the YbT_2Zn_{20} (T = Fe, Ru, Os, Ir, Rh, and Co) compounds are plotted in Fig. 2. In contrast to the isostructural Y-based compounds, $S(T)$ of the Yb-based compounds exhibits a large, negative minimum (between −75

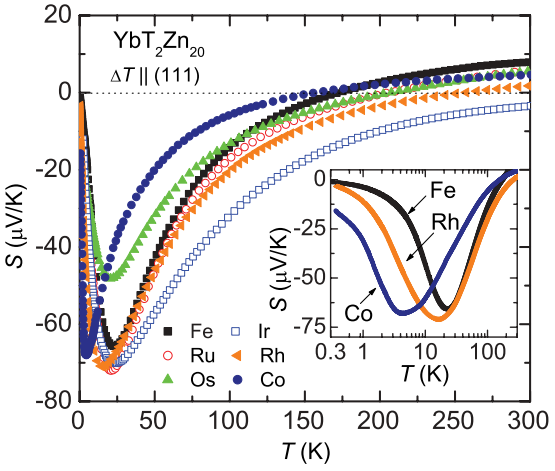

FIG. 2. (Color online) Temperature-dependent thermoelectric power, $S(T)$, of YbT_2Zn_{20} (T = Fe, Ru, Os, Ir, Rh, and Co) in zero applied magnetic field. Inset: $S(T)$ vs log(T) for T = Fe, Rh, and Co.

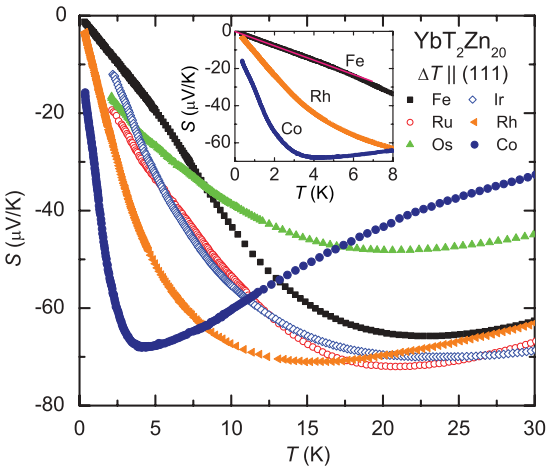

FIG. 3. (Color online) Low-temperature $S(T)$ of YbT_2Zn_{20} compounds in zero applied magnetic field. Inset: $S(T)$ for T = Fe, Rh, and Co below 8 K. Solid line on the top of the data for T = Fe is a guide to eye.

and −45 μV/K) and the sign of $S(T)$ changing above 150 K from negative to positive (not observed in this temperature range for T = Ir). The absolute TEP values of Yb-based compounds are much larger than Y-based compounds at low temperatures, whereas they have a similar order of magnitude compared to Y-based compounds around 300 K. A negative, highly enhanced value of the TEP, over the temperature region measured, is typical of those found in other Yb-based Kondo lattice systems.[24–26]

Figure 3 shows the low-temperature $S(T)$ of YbT_2Zn_{20}. For T = Fe and Ru, a broad minimum of $\sim$−70 μV/K is shown at the temperature $T^S_{min} \sim 22$ K. For T = Os, Ir, and Rh, a similar broad minimum develops at a temperature of $T^S_{min} \sim$ 16–23 K, where the width of the peak is wider than that for T = Fe and Ru. For T = Co, $S(T)$ shows a similar temperature dependence but with the minimum shifted to $T^S_{min} \sim 4$ K and it also shows slope changes around $\sim$1 and $\sim$8 K. The width of the minimum for T = Co is narrower than that for the other members of this family. Above 10 K, the absolute value of the TEP for T = Co reduces more rapidly as the temperature increases than it does for the other YbT_2Zn_{20} compounds and the sign of the TEP changes from negative to positive close to 150 K. For comparison, $S(T)$ curves for T = Co together with T = Fe and Rh are plotted on a semilogarithmic scale in the inset of Fig. 2. A smaller local minimum ($\sim$−48 μV/K) is observed for $YbOs_2Zn_{20}$. It is not clear at present if this is related to the electrical resistivity measurement that showed a larger residual resistivity in $YbOs_2Zn_{20}$ compared to other members (T = Fe, Ru, Ir, and Rh).[15] $S(T)$ of $YbIr_2Zn_{20}$ is negative over the whole temperature range measured, the sign change from negative to positive being expected around $\sim$400 K, based on a linear extrapolation of $S(T)$ above 250 K. Below 10 K (or 3 K for T = Co), $S(T)$ data for all compounds show a tendency of approaching zero and reveal linear temperature dependencies that, to varying degrees, approach $S(T) = \alpha T$. The inset of Fig. 3 shows data down to 0.4 K for T = Fe, Rh, and Co and shows roughly this linear behavior in greater detail.

The precise temperature dependence of $S(T)$ can be seen more quantitatively in Fig. 4 where the $S(T)/T$ of YbT_2Zn_{20}

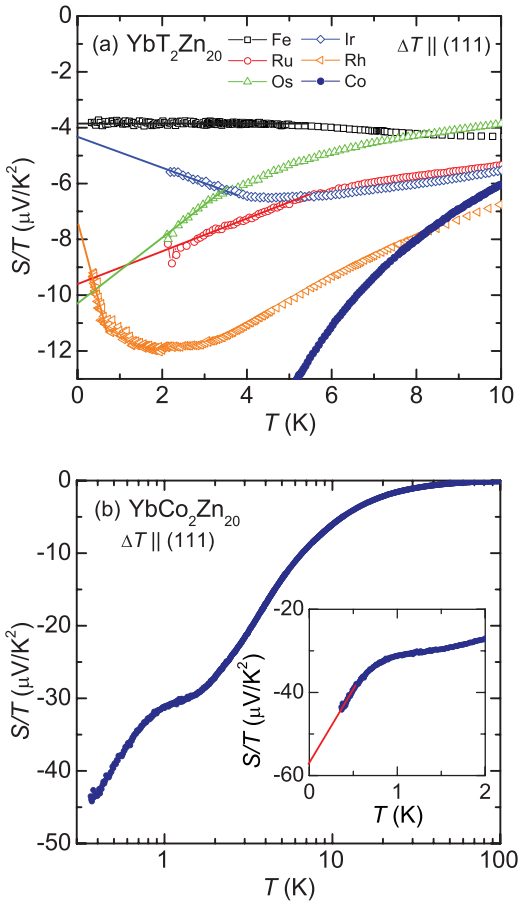

FIG. 4. (Color online) (a) $S(T)/T$ vs T for YbT_2Zn_{20} below 10 K in zero applied magnetic field. (b) $S(T)/T$ vs T for $YbCo_2Zn_{20}$ below 100 K. Inset: $S(T)/T$ vs T below 2 K. The solid lines represent the linear extrapolation curve to $T = 0$.

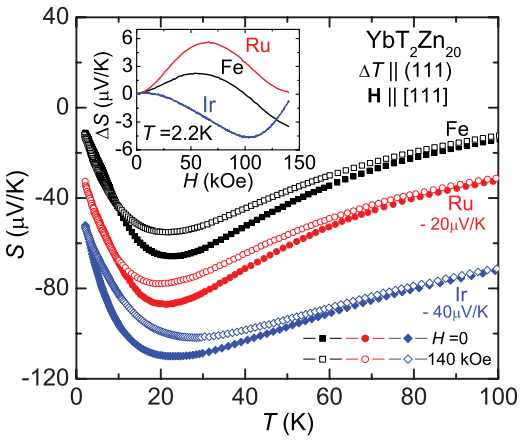

FIG. 5. (Color online) $S(T)$ of YbT_2Zn_{20} (T = Fe, Ru, and Ir) at $H = 0$ (closed symbols) and 140 kOe (open symbols). For clarity, the data for T = Ru and Ir are shifted by -20 and -40 μV/K, respectively. Inset: $\Delta S = S(H) - S(0)$ at 2.2 K for T = Fe, Ru, and Ir.

below 10 K is presented. For T = Fe the clear, linear temperature dependence of TEP, $S(T)/T = \alpha$, is revealed below 4 K. For other compounds, $S(T)/T$ shows an additional temperature dependence (probably due to the CEF effect and tiny phonon contribution). For T = Rh, the $S(T)/T$ shows a strong temperature dependence at low temperature which is consistent with the temperature dependence of $C(T)/T$,[15] where both $S(T)/T$ and $C(T)/T$ revealed a broad peak structure centered around 2–3 K. For T = Ir, the $S(T)/T$ and $C(T)/T$ also show a broad feature around 4 K. Similar linear $S(T)/T$ versus T (i.e., $S \propto T^2$) behavior was noted for the majority of HF compounds discussed in Ref. 13. This being said, the observed temperature dependence of $S(T)/T$ is not similar to the behavior shown in the resistivity, but is consistent with $C(T)/T$. The fact that the temperature region manifesting the Fermi-liquid behavior in the resistivity is not the same as that of the $S(T)/T$ can be due to several additional contributions to $S(T)$. Since the additional contributions cannot be completely separated, by using a first and simple approximation, the zero-temperature limit of $S(T)/T$ has been estimated by linearly extrapolating $S(T)$ from 2 K (or 0.4 K) to $T = 0$ (solid lines in Fig. 4), where the inferred $S(T)/T|_{T\to 0}$ values for T = Fe, Ru, Os, Ir, and Rh range between -3.8 and -10 μV/K^2. For T = Co, the $S(T)/T$ value at 0.4 K reaches -42 μV/K^2 and is still decreasing [see Fig. 4(b)]. By using a linear extrapolation, the $S(T)/T|_{T\to 0}$ value for T = Co is found to be ~ -57 μV/K^2.

In Fig. 5, the results of $S(T)$ measurements at $H = 0$ and 140 kOe are shown for T = Fe, Ru, and Ir. For clarity, the absolute value of the TEP is shifted by -20 μV/K for T = Ru and -40 μV/K for T = Ir. A slight change of $T^S_{\min}$ and a reduction of absolute value are seen for the H = 140 kOe data. Above 100 K, $S(T)$ for H = 140 kOe remains essentially the same as $S(T)$ for $H = 0$. In the zero-temperature limit for H = 140 kOe data, whereas $S(T)/T$ for T = Ru remains essentially the same, $S(T)/T$ at 140 kOe for T = Fe and Ir decreases from ~ -3.8 to ~ -6.4 μV/K^2 and from ~ -4 to ~ -6.6 μV/K^2, respectively. In the inset, the TEP measured at $T = 2.2$ K is plotted as a function of magnetic field for T = Fe, Ru, and Ir, where $\Delta S = S(H) - S(0)$. An interesting point of this result is the appearance of a maximum around $\sim$70 kOe for T = Fe and Ru and a minimum around $\sim$100 kOe for T = Ir. For T = Ir the local minimum field shown in TEP is roughly matched with the metamagneticlike anomaly seen around H = 120 kOe in magnetization isotherms, $M(H)$,[27] for **H** $\parallel$ [110]. For T = Fe and Ru the $M(H)$ data at T = 2 K do not show any signature of metamagneticlike behavior up to 70 kOe,[28] with $M(H)$ being linear in magnetic field for both compounds. In order to clarify this point, it is necessary to measure $M(H)$ for magnetic fields higher than 70 kOe, to see whether the anomaly in $S(H)$ is related to features in magnetization or electronic data.

IV. DISCUSSION

Based on earlier thermodynamic and transport measurements of this family,[15] $S(T)$ data for YbT_2Zn_{20} (T = Fe, Ru, Os, Ir, Rh, and Co) can be understood qualitatively by considering the Kondo (T_K) and CEF (Δ/k_B) effects. The compounds in this series appear to be a set of model Kondo lattice systems with varying energy scales: T_K and Δ/k_B. In Fig. 6(a), the Kondo temperature, T_K, determined from γ,[15] and the local minimum temperature, $T^S_{\min}$, observed in the zero

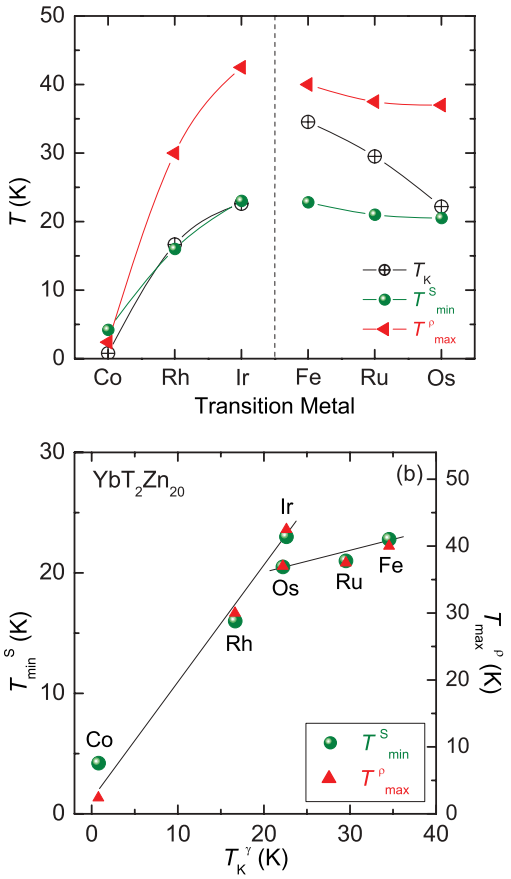

FIG. 6. (Color online) (a) Relevant characteristic temperatures in YbT_2Zn_{20} (T = Fe, Ru, Os, Ir, Rh, and Co). A Kondo temperature (T_K) calculated from γ, a local maximum temperature ($T^\rho_{\rm max}$) obtained from the resistivity, and a local minimum temperature ($T^S_{\rm min}$) developed in $S(T)$ are plotted as a function of transition metal. T_K^γ values are taken from Ref. 15. Vertical dashed line segregates two columns in the periodic table. (b) Plots of $T^S_{\rm min}$ (left) and $T^\rho_{\rm max}$ (right) vs T_K^γ. Solid lines are a guide to the eye.

field $S(T)$ data, are plotted as a function of the transition metal, T. The value of $T^S_{\rm min}$ correlates strongly with the value of T_K for T = Os, Ir, Rh, and Co.

A similar trend can be found in the previously published electrical resistivity, $\rho(T)$, results.[15] For T = Co, $\rho(T)$ manifests a clear local maximum, $T^\rho_{\rm max}$, around 2.4 K followed by a logarithmic temperature dependence as temperature decreases. Whereas $T^\rho_{\rm max}$ is clear in the $\rho(T)$ data for T = Co, $\rho(T)$ data from the other members of this family only show a clear local maximum after subtracting the resistivity data of the isostructural LuT_2Zn_{20} (T = Fe, Ru, Os, Ir, and Rh) compounds. The local maximum temperatures, $T^\rho_{\rm max}$, taken from Ref. 29 are plotted in Fig. 6(a). The variation of $T^\rho_{\rm max}$ follows the same trend as $T^S_{\rm min}$ with $T^\rho_{\rm max} \sim 2T^S_{\rm min}$ even for T = Fe and Ru.

In a Kondo lattice system, a single minimum developed in $S(T)$ is expected when T_K is either close to or higher than Δ/k_B. Typically, an intermediate valence system such as $YbAl_3$[24] and $YbCu_2Si_2$[25] and a fully degenerate Kondo lattice system such as $Yb_2Pt_6Al_{15}$[26] exhibit a single minimum in the TEP, developing below T_K. When $T_K < \Delta/k_B$, more than one peak has been frequently observed in the TEP.[25,30–32] The low-temperature extremum is usually located close to T_K, and the high-temperature extremum located at 0.4–0.6 Δ/k_B is attributed to Kondo scattering off of the thermally populated CEF levels, which is in agreement with theoretical predictions.[2,4,33–36] Therefore, the peak position can represent T_K and Δ/k_B as relevant energy scales in Kondo lattice systems.

For the YbT_2Zn_{20} family, T_K and the ground-state degeneracy play important roles in the thermodynamic and transport properties. By considering the ground-state degeneracy ($N = 8$ for T = Fe and Ru and $N = 4$ for T = Os, Rh, Ir, and Co[15]) it is expected that $T_K \geqslant \Delta/k_B$ for T = Fe and Ru and $T_K \lesssim \Delta/k_B$ for T = Os, Ir, Rh, and Co. Based on this, for T = Fe and Ru, it is reasonable to assume that $T^S_{\rm min}$ and $T^\rho_{\rm max}$ simply reflect T_K, with the fully degenerate case corresponding to $N = 8$. For T = Os, Ir, Rh, and Co, the two extrema in the $S(T)$ data associated with Kondo scattering on the ground state and thermally populated CEF levels could be expected; however, only one broad peak structure is developed for T = Os, Ir, Rh, and Co. We thus expect that a single broad minimum is produced by merging more than one peak structure due to the relatively small CEF level splitting ($T_K \sim \Delta/k_B$).

To reiterate, a strong correlation between the two local extrema $T^\rho_{\rm max}$ and $T^S_{\rm min}$ develops and remains robust even when dependence on T_K appears to break down [Fig. 6(b)]. $T^\rho_{\rm max} \sim 2\,T^S_{\rm min}$ for T = Fe, Ru, Os, Ir, and Rh, and for T = Os, Ir, Rh, and Co $T^S_{\rm min} \sim T_K$ and $T^\rho_{\rm max} \sim 2\,T_K$.

As shown in Fig. 5 the magnetic-field dependence of the TEP observed in YbT_2Zn_{20} (T = Fe, Ru, and Ir) is anomalous. In the simplest case of a two band model, the carrier density of electrons, n_e, and holes, n_h, can be taken as $\frac{1}{2}n = n_e = n_h$. The diffusion TEP in magnetic field with several assumptions[37] can be expressed as

$$\Delta S = S(H) - S(0) = -S(0)\frac{\Upsilon^2 H^2 \zeta(1+\zeta)}{1+\Upsilon^2 H^2 \zeta^2},$$

where $\Upsilon = 1/nec\rho(0)$, and $\zeta = L_n/L_0$ with $L_n = \frac{1}{3}(\pi k_B/e)^2$ and $L_0 = \kappa(0)/\sigma(0)T$ (Lorentz number); $\sigma(0) = 1/\rho(0)$ and $\kappa(0)$ are the electrical conductivity and thermal conductivity, respectively, in zero magnetic field. At low temperatures $L_0 = L_n$, $\rho(0) = \rho_0$ (the residual resistivity), and the diffusion TEP in zero magnetic field is proportional to the temperature, $S(0) \propto T$. Therefore, for simple metals $\Delta S = 0$ when $T = 0$, and for very low temperatures $\Delta S \propto T$. At high temperatures $L_0 = L_n$, and $S(0)$ and $\rho(0)$ are both proportional to temperature, so that ΔS tends to zero like $1/T$ as $T \to \infty$. In general, the change in the TEP will be too small to be detected at room temperature. Since the magnetoresistance (MR) for T = Fe and Ru is positive and increases monotonically at 2 K for $\mathbf{H} \parallel [111]$ up to 140 kOe,[29] the change of the TEP (ΔS) should increase or saturate with increasing magnetic field. The field dependence of the TEP is not consistent with the MR results. Generally, the phonon drag itself is not sensitive to the applied magnetic field,[21] so it is clear that neither conventional phonon drag nor diffusion TEP of conduction electrons can account for the magnetic field dependence of the TEP in these compounds. Thus, multiple factors, such as the Kondo effect and CEF contributions, have to be considered. In order to

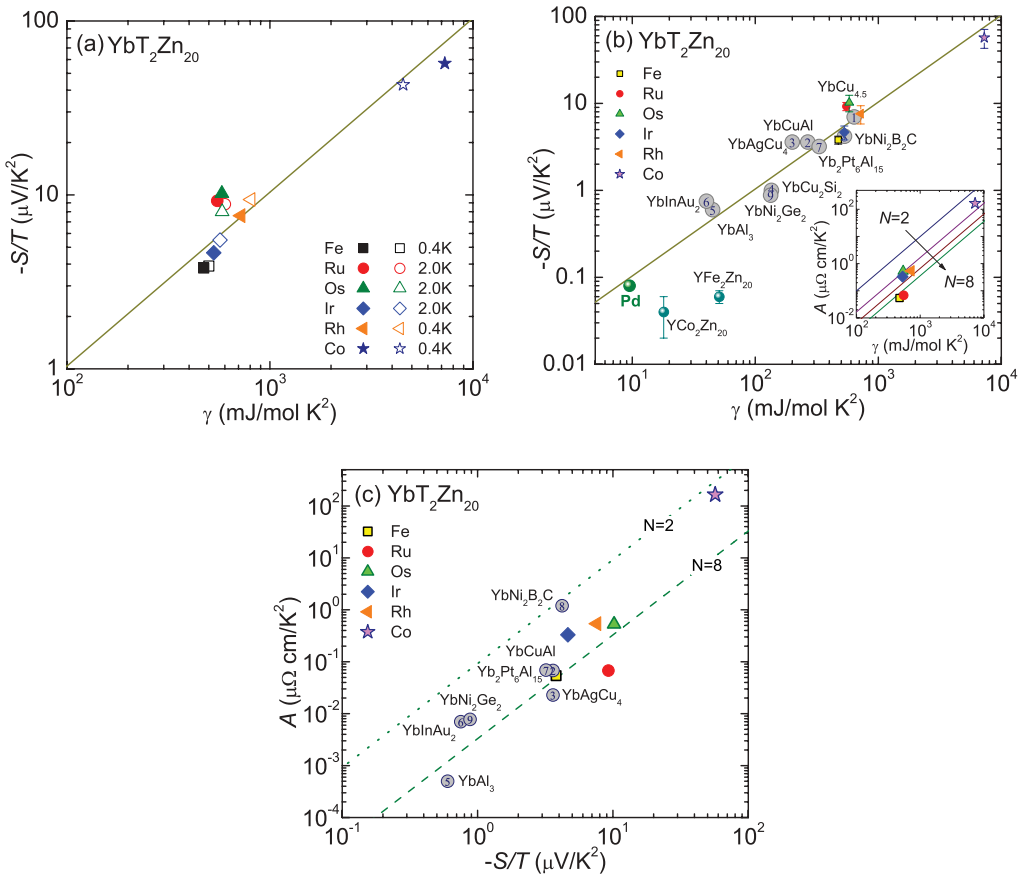

FIG. 7. (Color online) (a) $-S(T)/T$ vs γ (log-log) plot of YbT_2Zn_{20} (T = Fe, Ru, Os, Ir, Rh, and Co). Solid symbols are obtained by the linear extrapolation of $-S(T)/T|_{T\to 0}$ and $\gamma \equiv C(T)/T|_{T\to 0}$. Open symbols are taken by the value of $S(T)/T$ and $C(T)/T$ at base temperature measured (0.4 K for T = Fe, Rh, and Co and 2 K for T = Ru, Os, and Ir). (b) $-S(T)/T|_{T\to 0}$ vs γ (log-log) plot of YbT_2Zn_{20} with reported compounds. The zero-temperature limits of $S(T)/T$ and γ for (1) $YbCu_{4.5}$, (2) YbCuAl, (3) $YbAgCu_4$, (4) $YbCu_2Si_2$, (5) $YbAl_3$, (6) $YbInAu_2$, and Pd are taken from the table of Ref. 13, $S(T)/T$ and γ of (7) $Yb_2Pt_6Al_{15}$ are taken from Ref. 26, and $S(T)/T$ and γ of (8) $YbNi_2B_2C$ and (9) $YbNi_2Ge_2$ are taken from Refs. 42–44, respectively. The solid line represents $\gamma/(eN_A)$. Inset: Kadowaki-Woods plot (log-log plot of A vs γ) of YbT_2Zn_{20}. Symbols are taken from Ref. 15 and solid lines correspond to N = 2, 4, 6, and 8 based on Ref. 9, respectively. (c) A vs $-S(T)/T$ (log-log) plot for Yb-based compounds. $S(T)/T$ values are the same as in (b) and A values are taken from Refs. 7,15,26, and 44. The dotted and dashed lines are the $A \sim S/T^2$ lines for N = 2 and 8, respectively. See details in text.

understand the observed behavior in more detail, a theoretical analysis of the TEP as a function of field for these systems will be necessary.

Earlier thermodynamic and transport measurements[15] showed that the R_W and K-W ratios of YbT_2Zn_{20} agree well with the FL picture of the HF ground state. A clear dependence of the A/γ^2 ratio on the degeneracy N is shown in the inset of Fig. 7(b), where the A and γ values are taken from Ref. 15 and lines for degeneracies N are based on Ref. 9. A Fermi-liquid state can also be characterized by the ratio between γ and the zero-temperature limit of $S(T)/T$:[13,38,39] a "quasiuniversal" ratio $q = N_A eS/\gamma T$ remains close to $q = \pm 1$ for metals and the sign of q depends on the type of carriers. Although for strongly correlated electronic materials like HF systems, a single band and single scattering process is not generally thought to be sufficient for explaining the strong correlation effects, given that $C(T)/T$ and $S(T)/T$ are most sensitive to the position of the heavy band, a quasiuniversal ratio is expected to hold at low temperatures.[40,41]

As shown in Figs. 1 and 4, a clear Fermi-liquid behavior, $S(T)/T = \alpha$, is shown for YFe_2Zn_{20} and $YbFe_2Zn_{20}$. The other compounds in this family reveal a deviation from the linear temperature dependence of TEP within the measured temperature range, where the feature shown in temperature dependence $S(T)/T$ is similar to that of $C(T)/T$. Since several effects in $S(T)/T$ are included, such as CEF and phonon contribution, $S(T)/T$ vs $C(T)/T$ is compared both at finite temperature and the zero-temperature limit (the latter being the same approach used for the majority of HF systems shown in Fig. 1 of Ref. 13). In Fig. 7(a), $S(T)/T$ at lowest temperature measured vs $C(T)/T$ is plotted, at 0.4 K for T = Fe, Rh, Co and 2 K for T = Ru, Os, Ir, as shown by open symbols. The zero-temperature limit of $S(T)/T$, estimated by simple linear extrapolation of $S(T)/T$ from 2 K (or 0.4 K) to T = 0 [solid lines in Fig. 4(a)], is also plotted [closed symbols in Fig. 7(a)]. Both the zero-temperature limit and $S(T)/T$ value at the lowest temperature measured are locating close to the line with $q = -1$.

The experimental correlation between the zero-temperature limit of $S(T)/T$ and γ for YbT_2Zn_{20} (T = Fe, Ru, Os, Ir, Rh, and Co) and YT_2Zn_{20} (T = Fe and Co) is presented in Fig. 7(b). Though error bars cannot be determined exactly from the present data because additional contributions such as phonon and CEF effect in $S(T)/T$ cannot be completely separated, one can use the difference between the base temperature value measured and the extrapolated value to $T = 0$. The error bars in Fig. 7(b) are based on the difference between the values determined from the base temperature value measured and linear extrapolation to $T = 0$ [other experimental error has not been applied to the error bar in Fig. 7(b), where the experimental error is smaller than the error bar determined]. Given that Fig. 7(b) is a log-log plot, spanning orders of magnitude, the error bars are of limited concern. For comparison, data for several other Yb-based HF compounds as well as Pd are also plotted in the same figure.[42] The calculated q values of Yb-based compounds vary from -0.77 for T = Fe to -1.4 for T = Rh, which are close to the value $q = -1$, expected for holelike charge carriers.

As shown in Fig. 7(b), each Yb-based data point is close to a line represented by $q = -1$ which means that the zero-temperature limit of $S(T)/T$ is strongly correlated to γ due to the enhanced density of state at the Fermi level; the larger density of states at the Fermi level results in a larger γ and $S(T)/T|_{T\to 0}$. For YFe_2Zn_{20} and YCo_2Zn_{20}, though, the calculated q (~ -0.1) value is ten times smaller than that for the free electron case. This can be understood, at least in part, by appreciating the fact that, since the γ term is not dominated by a huge Yb contribution, the γ value should probably be expressed in per-mole-atomic terms, reduced by a factor of $\sim$20. Such a reduction of γ would place these two data points more or less on the $q = -1$ line.

Given the large range of $S(T)/T$ and γ values found for the YbT_2Zn_{20} compounds we can examine the direct correlation found between $S(T)/T$ and A for Yb-based materials. In Fig. 7(c), data from Refs. 7 and 26 along with our data for the six YbT_2Zn_{20} compounds are shown. At the grossest level, larger $S(T)/T$ values correspond to larger A values. More quantitatively, in a naive picture, since $A \propto \gamma^2$ and $S(T)/T \propto \gamma$, then $A \propto (S(T)/T)^2$. In Fig. 7(c), the dotted and dashed lines are the $A \sim (S/T)^2$ lines with prefactors appropriate for $N = 2$ and 8, respectively, discussed for the generalized K-W ratio; $A/(S/T)^2 = 9.216 \times 10^4/(0.5N(N-1)\ \Omega\ \mathrm{cm/K^2/(C/mol\ V/K)^2}$, where $A/\gamma^2 = 1.0 \times 10^{-5}/(0.5N(N-1)\ \Omega\ \mathrm{cm/(J/mol\ K)^2}$[29] and $q = -1$[13] are used. As can be seen, virtually all of the data, for a diverse set of structures, Kondo temperatures, and Yb content, fall between these two extremes, simultaneously (1) giving some sense that they are capturing the salient correlation between these values and (2) demanding a more detailed and formal, theoretical examination of the relation between these two transport properties in strongly correlated electron systems.

V. SUMMARY

The thermoelectric power measurements on the YbT_2Zn_{20} (T = Fe, Ru, Os, Ir, Rh, and Co) compounds are in agreement with the behavior observed in many heavy fermion Kondo lattice systems. The evolution of the local minimum in $S(T)$ and the local maximum (coherence temperature) in $\rho(T)$ with variation of the transition metals can be understood based on the energy scale of Kondo temperature in conjunction with the influence of the crystalline electric field splitting. The large value of $S(T)/T$ in the zero-temperature limit can be scaled with the electronic specific heat coefficient, γ, which is reflected by a strong correlation via the universal ratio $q = N_A eS/\gamma T$ and confirms the validity of Fermi-liquid descriptions. In addition, for a wide range of Yb-based materials there is a clear, apparently simple, correlation between $S(T)/T$ and A.

ACKNOWLEDGMENTS

This work was supported by the US Department of Energy, Office of Basic Energy Science, Division of Materials Sciences and Engineering. The research was performed at the Ames Laboratory. The Ames Laboratory is operated for the US Department of Energy by Iowa State University under Contract No. DE-AC02-07CH11358.

*Current address: National High Magnetic Field Laboratory, Los Alamos National Laboratory, Los Alamos, NM 87545, USA.

†Current address: Department of Chemistry, Princeton University, Princeton, NJ 08544, USA.

[1] A. C. Hewson, *Kondo Problem to Heavy Fermion* (Cambridge University Press, Cambridge, 1993).

[2] A. K. Bhattacharjee and B. Coqblin, Phys. Rev. B **13**, 3441 (1976).

[3] Y. Lassailly, A. K. Bhattacharjee, and B. Coqblin, Phys. Rev. B **31**, 7424 (1985).

[4] S. Maekawa, S. Kashiba, M. Tachiki, and S. Takahashi, J. Phys. Soc. Jpn. **55**, 3194 (1986).

[5] K. Kadowaki and S. B. Woods, Solid State Commun. **58**, 507 (1986).

[6] K. Miyake, T. Matsuura, and C. M. Varma, Sold State Commun. **71**, 1149 (1989).

[7] N. Tsujii, K. Yoshimura, and K. Kosuge, J. Phys.: Condens. Matter **15**, 1993 (2003).

[8] H. Kontani, J. Phys. Soc. Jpn. **73**, 515 (2004).

[9] N. Tsujii, H. Kontani, and K. Yoshimura, Phys. Rev. Lett. **94**, 057201 (2005).

[10] P. B. Weigman and A. M. Tsvelik, J. Phys. C: Solid State Phys. **16**, 2281 (1983); **16**, 2321 (1983).

[11] A. Auerbach and K. Levin, Phys. Rev. B **34**, 3524 (1986).

[12] P. A. Lee, T. M. Rice, J. W. Serene, L. J. Sham, and J. W. Wilkins, Comments Condens. Matter Phys. **12**, 99 (1986).

[13] K. Behnia, D. Jaccard, and J. Flouquet, J. Phys.: Condens. Matter **16**, 5187 (2004).

[14] V. M. T. Thiede, W. Jeitschko, S. Niemann, and T. Ebel, J. Alloys Compd. **267**, 23 (1998).

[15]M. S. Torikachvili, S. Jia, E. D. Mun, S. T. Hannahs, R. C. Black, W. K. Neils, D. Martien, S. L. Bud'ko, and P. C. Canfield, Proc. Natl. Acad. Sci. USA **104**, 9960 (2007).
[16]S. Jia, S. L. Bud'ko, G. D. Samolyuk, and P. C. Canfield, Nat. Phys. **3**, 334 (2007).
[17]P. C. Canfield and Z. Fisk, Philos. Mag. B **65**, 1117 (1992).
[18]P. C. Canfield, *Solution Growth of Intermetallic Single Crystals*: *A Beginner's Guide*, Book Series on Complex Metallic Alloys (World Scientific, Singapore, 2010).
[19]E. Mun, S. L. Bud'ko, M. S. Torikachvili, and P. C. Canfield, Meas. Sci. Technol. **21**, 055104 (2010).
[20]S. Jia, N. Ni, G. D. Samolyuk, A. Safa-Sefat, K. Dennis, Hyunjin Ko, G. J. Miller, S. L. Bud'ko, and P. C. Canfield, Phys. Rev. B **77**, 104408 (2008). Note that the Debye temperatures used in this paper are recalculated: Θ_D (YFe_2Zn_{20}) = 350 K and Θ_D (YCo_2Zn_{20}) = 344 K.
[21]F. J. Blatt, P. A. Schroeder, C. L. Foiles, and D. Greig, *Thermoelectric Power of Metals* (Plenum, New York, 1976); F. J. Blatt, A. D. Caplin, C. K. Chiang, and P. A. Schroeder, Solid State Commun. **15**, 411 (1974).
[22]T. Takabatake, E. Matsuoka, S. Narazu, K. Hayashi, S. Morimoto, T. Sasakawa, K. Umeo, and M. Sera, Physica B **383**, 93 (2006).
[23]E. Gratz and A. S. Markosyan, J. Phys.: Condens. Matter **13**, R385 (2001).
[24]C. L. Foiles, J. Appl. Phys. **52**, 2217 (1981).
[25]D. Andreica, K. Alami-Yadri, D. Jaccard, A. Amato, and D. Schenck, Physica B **259–261**, 144 (1999).
[26]M. Deppe, S. Hartmann, M. E. Macovei, N. Oeschler, M. Nicklas, and C. Geibel, New J. Phys. **10**, 093017 (2008).
[27]S. Yoshiuchi, M. Toda, M. Matsushita, S. Yasui, Y. Hirose, M. Ohya, K. Katayama, F. Honda, K. Sugiyama, M. Hagiwara, K. Kindo, T. Takeuchi, E. Yamamoto, Y. Haga, R. Settai, T. Tanaka, Y. Kubo, and Y. Onuki, J. Phys. Soc. Jpn. **78**, 123711 (2009).
[28]E. Mun (unpublished).
[29]E. Mun, Ph. D. thesis, Iowa State University, 2010. In zero field, the resistivity data for YbT_2Zn_{20} compounds were taken from Ref. 15. The resistivity data for $LuFe_2Zn_{20}$ and $LuCo_2Zn_{20}$ compounds were taken from S. Jia, N. Ni, S. L. Bud'ko, and P. C. Canfield, Phys. Rev. B **80**, 104403 (2009). The resistivity data for LuT_2Zn_{20} (T = Ru, Os, Ir, and Rh) are unpublished.
[30]D. Huo, J. Sakurai, O. Maruyama, T. Kuwai, and Y. Isikawa, J. Magn. Magn. Mater. **226–230**, 202 (2001).
[31]H. Wilhelm and D. Jaccard, Phys. Rev. B **69**, 214408 (2004).
[32]U. Köhler, N. Oeschler, F. Steglich, S. Maquilon, and Z. Fisk, Phys. Rev. B **77**, 104412 (2008).
[33]N. E. Bickers, D. L. Cox, and J. W. Wilkins, Phys. Rev. Lett. **54**, 230 (1985).
[34]G. D. Mahan, Phys. Rev. B **56**, 11833 (1997).
[35]V. Zlatić, B. Horvatić, I. Milat, B. Coqblin, G. Czycholl, and C. Grenzebach, Phys. Rev. B **68**, 104432 (2003).
[36]V. Zlatić and R. Monnier, Phys. Rev. B **71**, 165109 (2005).
[37]E. H. Sondheimer, Proc. R. Soc. London A **193**, 484 (1948).
[38]C. Grenzebach, F. B. Anders, G. Czycholl, and T. Pruschke, Phys. Rev. B **74**, 195119 (2006).
[39]V. Zlatić, R. Monnier, J. K. Freericks, and K. W. Becker, Phys. Rev. B **76**, 085122 (2007).
[40]K. Miyake and H. Kohno, J. Phys. Soc. Jpn. **74**, 254 (2005).
[41]H. Kontani, Phys. Rev. B **67**, 014408 (2003).
[42]The zero-temperature limit of S/T and γ for YbCuAl, $YbInAu_2$, $YbAl_3$, $YbCu_2Si_2$, $YbAgCu_4$, and $YbCu_{4.5}$ are taken from the table of Ref. 13. S/T and γ of $Yb_2Pt_6Al_{15}$ are taken from Ref. 26. The γ values of $YbNi_2B_2C$ and $YbNi_2Ge_2$ are taken from Refs. 43 and 44, respectively. The TEP data of $YbNi_2B_2C$ and $YbNi_2Ge_2$ are taken from Ref. 29.
[43]S. Li, M. C. De Andrade, E. J. Freeman, C. Sirvent, R. P. Dickey, A. Amann, N. A. Frederick, K. D. D. Rathnayaka, D. G. Naugle, S. L. Bud'ko, P. C. Canfield, W. P. Beyermann, and M. B. Maple, Philos. Mag. B **86**, 3021 (2006).
[44]S. L. Bud'ko, Z. Islam, T. A. Wiener, I. R. Fisher, A. H. Lacerda, and P. C. Canfield, J. Magn. Magn. Mater. **205**, 53 (1999).